Threshold neutral pion photoproduction off the tri-nucleon to $\mathcal{O}(q^4)$

Mark Lenkewitz[⋆#1], Evgeny Epelbaum[⋆#2], H.-W. Hammer[⋆#3] and Ulf-G. Meißner[⋆‡#4]

[⋆] *Universität Bonn, Helmholtz–Institut für Strahlen– und Kernphysik (Theorie) and Bethe Center for Theoretical Physics, D-53115 Bonn, Germany*

[⋆] *Ruhr-Universität Bochum, Institut für Theoretische Physik II D-44870 Bochum, Germany*

[‡] *Forschungszentrum Jülich, Institut für Kernphysik (IKP-3), Institute for Advanced Simulation (IAS-4) and Jülich Center for Hadron Physics D-52425 Jülich, Germany*

Abstract

We calculate electromagnetic neutral pion production off tri-nucleon bound states (^{3}H, ^{3}He) at threshold in chiral nuclear effective field theory to fourth order in the standard heavy baryon counting. We show that the fourth order two-nucleon corrections to the S-wave multipoles at threshold are very small. This implies that a precise measurement of the S-wave cross section for neutral pion production off ^{3}He allows for a stringent test of the chiral perturbation theory prediction for the S-wave electric multipole $E_{0+}^{\pi^0 n}$.

[#1] email: lenkewitz@hiskp.uni-bonn.de
[#2] email: evgeny.epelbaum@rub.de
[#3] email: hammer@hiskp.uni-bonn.de
[#4] email: meissner@hiskp.uni-bonn.de

1 Introduction

In the absence of free neutron targets, light nuclei like the deuteron or three-nucleon bound states like ^{3}H (triton) or ^{3}He can be used to unravel the properties of neutrons. For a recent review on extracting the neutron structure from electron or photon scattering off light nuclei, see Ref. [1]. Of particular interest in this respect is threshold neutral pion photo- and electroproduction off the nucleon. This is one of the finest reactions to test the chiral dynamics of QCD, see Ref. [2] for a recent review. Arguably most striking is the counterintuitive chiral perturbation theory prediction (CHPT) that the elementary neutron S-wave multipole $E_{0+}^{\pi^0 n}$ is larger in magnitude than the corresponding one of the proton, $E_{0+}^{\pi^0 p}$ [3, 4]. This prediction was already successfully tested in neutral pion photo- [5, 6] and electroproduction off the deuteron [7]. However, given the scarcity and precision of the corresponding data, it is mandatory to study also pion production off tri-nucleon bound states, that can be calculated nowadays to high precision based on chiral nuclear effective field theory (EFT). This framework extends CHPT to nuclear physics (for recent reviews, see [8, 9]). ^{3}He appears to be a particularly promising target to extract information about the neutron amplitude. This idea is usually invoked for spin-dependent quantities since the ^{3}He wave function is strongly dominated by the principal S-state component which suggests that its spin is largely driven by the one of the neutron. The photo- and electroproduction of neutral pions from tri-nucleon systems (^{3}He and ^{3}H) was considered in Ref. [10] based on chiral 3N wave functions at next-to-leading order in the standard heavy baryon expansion. Here, we extend this calculation to fourth order in the chiral expansion, including consistently *all* next-to-next-to-leading order contributions in the standard heavy baryon expansion. This amounts to a complete (i.e. subleading) one-loop calculation in the one-nucleon sector. An investigation of the role of nucleon recoil, accounting for the scale $\chi = \sqrt{M_\pi m_N} \simeq 340$ MeV, is beyond the scope of this work and will be left for the future.

Experimentally, neutral pion photoproduction off light nuclei has so far only been studied at Saclay [11,12] and at Saskatoon [13,14]. Clearly, new measurements using CW beams, modern targets and detectors are urgently called for. The results presented below show that we are able to calculate neutral pion photoproduction off tri-nucleon systems to very good precision and, moreover, that the S-wave cross section for neutral pion production off ^{3}He is very sensitive to the elementary $E_{0+}^{\pi^0 n}$ multipole (as already stressed in Ref. [10]).

Our manuscript is organized as follows. Section 2 contains all the necessary formalism. In particular, we spell out in detail the fourth order two-nucleon corrections that modify the third order results of Ref. [10]. We also briefly recall the contributions worked out in that paper. Section 3 contains our results and the discussion of these. We end with a short summary and outlook in Sec. 4.

2 Formalism

2.1 Generalities

Pion production off a tri-nucleon bound state is given in terms of three different topologies of Feynman diagrams, see Fig. 1. While the single-nucleon contribution (a) corresponding to the standard impulse approximation features the elementary neutron and proton production amplitudes, the nuclear corrections are given by two-body (b) and three-body (c) terms. Based on the power counting developed in [5], at next-to-next-to-leading order (NNLO), only the topologies (a) and (b) contribute. Topology (c) starts to contribute at fourth order to P-wave multipoles and is thus not of relevance for our considerations. Here, we will specifically consider threshold photo- and electroproduction parameterized in terms of the electric E_{0+} and longitudinal L_{0+} S-wave multipoles. In particular, we study the sensitivity of the ^{3}H/^{3}He S-wave multipoles to the elementary $E_{0+}^{\pi^0 n}$ multipole, as the production

amplitude off the proton is well understood experimentally and theoretically.

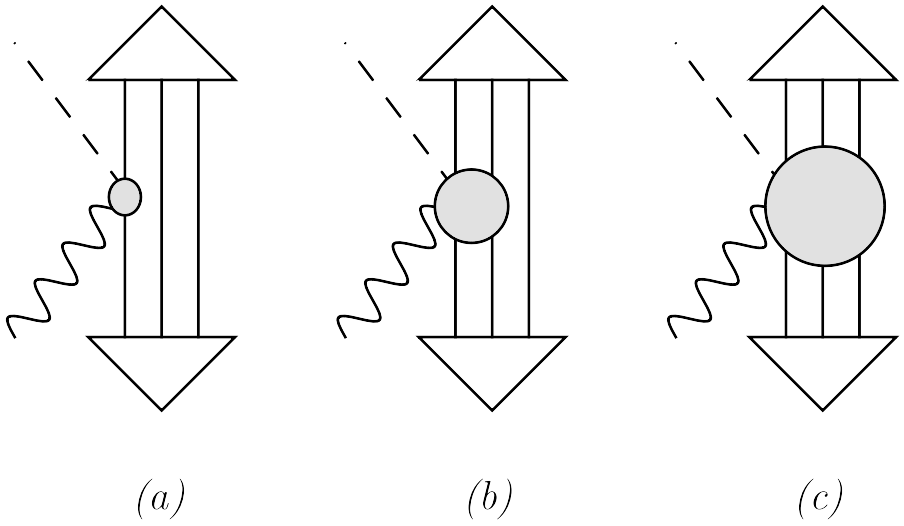

Figure 1: Different topologies contributing to pion production off the three-nucleon bound state (triangle). (a), (b) and (c) represent the single-, two- and three-nucleon contributions, respectively. Solid, dashed and wiggly lines denote nucleons, pions and photons, in order. Topology (c) does not contribute to the order considered here (NNLO).

To analyze pion photo- and electroproduction of the tri-nucleon system, one has to calculate the nuclear matrix element of the transition operator $\hat{O}$ as:

$$\langle M_J' | \hat{O} | M_J \rangle_\psi := \langle \psi \, M_J' \, \vec{P}_{3N}' \, \vec{q} \, | \, \hat{O} \, | \, \psi \, M_J \, \vec{P}_{3N} \, \vec{k} \, \rangle \, , \tag{1}$$

where ψ refers to the three-nucleon state and $\vec{k}$, $\vec{q}$, $\vec{P}_{3N}$ and $\vec{P}_{3N}'$ denote the momentum of the real or virtual photon, produced pion and the initial and final momenta of the 3N nucleus, respectively. We use the Coulomb gauge throughout this work. Note, however, that the Coulomb gauge condition is only satisfied up to higher order corrections in our calculation. Possible improvements are discussed in Refs. [15, 16].

The 3N bound state has total nuclear angular momentum $J = 1/2$ with magnetic quantum numbers M_J for the initial and M_J' for the final nuclear state. J can be decomposed in total spin $S = 1/2, 3/2$ and total orbital angular momentum $L = 0, 1, 2$. The total isospin is a mixture of two components, $T = 1/2$ and $3/2$. While the $T = 1/2$ component is large, the small $T = 3/2$ component emerges due to isospin breaking and is neglected in our calculation. The isospin magnetic quantum numbers are $M_T = M_{T'} = 1/2$ for ^{3}He and $M_T = M_{T'} = -1/2$ for ^{3}H. In this paper, we consider neutral pion production by real or virtual photons off a spin-1/2 particle - either the nucleon or the ^{3}H and ^{3}He nuclei. At threshold, the corresponding transition matrix takes the form

$$\mathcal{M}_\lambda = 2i \, E_{0+} \, (\vec{\epsilon}_{\lambda,\mathrm{T}} \cdot \vec{S}) + 2i \, L_{0+} \, (\vec{\epsilon}_{\lambda,\mathrm{L}} \cdot \vec{S}) \, , \tag{2}$$

with $\vec{\epsilon}_{\lambda,\mathrm{T}} = \vec{\epsilon}_\lambda - (\vec{\epsilon}_\lambda \cdot \hat{k}) \hat{k}$ and $\vec{\epsilon}_{\lambda,\mathrm{L}} = (\vec{\epsilon}_\lambda \cdot \hat{k}) \hat{k}$ the transverse and longitudinal photon polarization vectors, and $\vec{S}$ is the spin vector. The transverse and longitudinal S-wave multipoles are denoted by E_{0+} and L_{0+}, respectively. Note that L_{0+} contributes only for virtual photons. Also, as will be explained later in more detail, due to boost effects that appear at next-to-next-to-leading order (NNLO), there will be P-wave corrections to the S-wave multipoles. In the following, we will first recapitulate the leading one-loop calculation from Ref. [10] and then systematically work out the NNLO corrections.

The chiral expansion of the pertinent amplitudes is done in complete analogy to the case of the deuteron discussed in detail in Ref. [6]. We summarize here only briefly the most important issues. First, the production operator on the single nucleon is worked out to fourth order in the chiral expansion. This is consistent with the two-body contributions (exchange currents) worked out here. The leading two-nucleon terms start at third order and have been evaluated in Ref. [10]. At fourth order, there are further corrections to the two-body currents which can be classified as boost, static and recoil contributions. These will be worked out in detail in the following paragraphs. Second, using the same arguments as in Ref. [5,6], one can show that there are no contributions from short-distance four-nucleon-pion-photon operators at threshold (which is the case we consider here). Notice that such operators do contribute at fourth order for nonvanishing momenta of the produced pion.

2.2 Single nucleon and leading two-nucleon contributions at threshold

As explained before, the matrix element Eq. (1) receives contributions from one- and two-nucleon operators at the order we are working. Consider first the single nucleon contribution, given in terms of the 1-body transition operator $\hat{O}^{\rm 1N}$. After some algebra, one finds

$$\langle M_J'|\hat{O}^{\rm 1N}|M_J\rangle_\psi = i\vec{\epsilon}_{\lambda,\rm T}\cdot\vec{S}_{M_J'M_J}\Big(E_{0+}^{\pi^0 p}F_T^{S+V}+E_{0+}^{\pi^0 n}F_T^{S-V}\Big)+i\vec{\epsilon}_{\lambda,\rm L}\cdot\vec{S}_{M_J'M_J}\Big(L_{0+}^{\pi^0 p}F_L^{S+V}+L_{0+}^{\pi^0 n}F_L^{S-V}\Big)\ , \tag{3}$$

where $F_{T/L}^{S\pm V}\equiv F_{T/L}^S\pm F_{T/L}^V$ and $F_{T/L}^{S,V}$ denote the corresponding form factors of the 3N bound state,

$$\begin{aligned} F_{T/L}^S\,\vec{\epsilon}_{\lambda,\rm T/L}\cdot\vec{S}_{M_J'M_J} &= \frac{3}{2}\,\langle M_J'|\vec{\epsilon}_{\lambda,\rm T/L}\cdot\vec{\sigma}_1|M_J\rangle_\psi\ , \\ F_{T/L}^V\,\vec{\epsilon}_{\lambda,\rm T/L}\cdot\vec{S}_{M_J'M_J} &= \frac{3}{2}\,\langle M_J'|\vec{\epsilon}_{\lambda,\rm T/L}\cdot\vec{\sigma}_1\tau_1^z|M_J\rangle_\psi\ , \end{aligned} \tag{4}$$

which parameterize the response of the composite system to the excitation by photons in spin-isospin space. $\vec{S}_{M_J'M_J}$ are the corresponding spin transitions matrix elements. In the above equation, $\vec{\sigma}_i$ ($\vec{\tau}_i$) denote the spin (isospin) Pauli matrices corresponding to the nucleon i. Furthermore, z refers to the isospin quantization axis.

Using the 3N wave functions from chiral nuclear EFT at the appropriate order, the pertinent matrix elements in Eq. (4) can be evaluated. Here, we use chiral 3N wave functions obtained from the N^{2}LO interaction in the Weinberg power counting [17,18].[#5] In order to estimate the error from higher order corrections, we use wave functions for five different combinations of the cutoff $\tilde{\Lambda}$ in the spectral function representation of the two-pion exchange and the cutoff Λ used to regularize the Lippmann-Schwinger equation for the two-body T-matrix. The wave functions are taken from Ref. [19, 20] and the corresponding cutoff combinations in units of MeV are $(\tilde{\Lambda},\Lambda)$ = (450,500), (600,500), (550,600), (450,700), (600,700). All five sets describe the binding energies of the ^{3}He and ^{3}H nuclei equally well (after inclusion of the corresponding three-nucleon force).

The one-body contribution to the 3N multipoles are given by

$$\begin{aligned} E_{0+}^{\rm 1N} &= \frac{K_{\rm 1N}}{2}\left(E_{0+}^{\pi^0 p}\,F_T^{S+V}+E_{0+}^{\pi^0 n}\,F_T^{S-V}\right)\ , \\ L_{0+}^{\rm 1N} &= \frac{K_{\rm 1N}}{2}\left(L_{0+}^{\pi^0 p}\,F_L^{S+V}+L_{0+}^{\pi^0 n}\,F_L^{S-V}\right)\ . \end{aligned} \tag{5}$$

[#5] The consistency of the Weinberg counting for short-range operators and the non-perturbative renormalization of chiral EFT are currently under discussion, see the reviews [8,9] and references therein for more details. A real alternative to the Weinberg approach for practical calculations in systems of three and more nucleons, however, is not available.

nucleus	^{3}He	^{3}H
F_T^{S+V}	0.017(13)(3)	1.493(25)(3)
F_T^{S-V}	1.480(26)(3)	0.012(13)(3)
F_L^{S+V}	−0.079(14)(8)	1.487(27)(8)
F_L^{S-V}	1.479(26)(8)	−0.083(14)(8)

Table 1: Numerical results for the form factors $F_{T/L}^{S\pm V}$. The first error is our estimation of the theoretical uncertainty resulting from the truncation of the chiral expansion while the second one is the statistical error from the Monte Carlo integration.

Here, K_{1N} is the kinematical factor to account for the change in phase space from the 1N to the 3N system,

$$K_{\rm 1N} = \frac{m_N + M_\pi}{m_{\rm 3N} + M_\pi} \frac{m_{\rm 3N}}{m_N} \approx 1.092\,, \tag{6}$$

with m_N being the nucleon mass and $m_{\rm 3N}$ the mass of the three-nucleon bound state. Throughout, we denote the neutral pion mass by M_π, but the S-wave multipoles are usually given in terms of the charged pion mass M_{π^+} and also the charged pion mass appears in some of the two-nucleon contributions.

We evaluate the matrix elements for the one-body contribution in Eq. (4) numerically with Monte Carlo integration using the VEGAS algorithm [21]. The results for the form factors $F_{T/L}^{S\pm V}$ are given in Table 1. The first error represents the theoretical uncertainty estimated from the cutoff variation in the wave functions. We take the central value defined by the five different cutoff sets as our prediction and estimate the theory error from higher-order corrections from the spread of the calculated values. Strictly speaking, this procedure gives a lower bound on the error, but in practice it generates a reasonable estimate. The second error is the statistical error from the Monte Carlo evaluation of the integrals. It is typically much smaller than the estimated theory error and can be neglected. Note that the single nucleon results in Table 1 are consistent with isospin symmetry within the numerical accuracy. This feature was not explicitly enforced and provides a check on our calculation.

We stress that we follow the nuclear EFT formulation of Lepage, in which the whole effective potential is iterated to all orders when solving the Schrödinger equation for the nuclear states. As discussed in Ref. [22], the cutoff should be kept of the order of the breakdown scale or below in order to avoid unnatural scaling of the coefficients of higher order terms. Indeed, using larger cutoffs can lead to a violation of certain low-energy theorems as demonstrated in Ref. [23] for an exactly solvable model.

The error related to the expansion of the production operator is difficult to estimate given that the convergence in the expansion for the single nucleon S-wave multipoles is known to be slow, see Ref. [3] for an extended discussion. We therefore give only a rough estimate of this uncertainty. The extractions of the proton S-wave photoproduction amplitude based on CHPT using various approximations [24] lead to an uncertainty $\Delta E_{0+}^{\pi^0 p} \approx \pm 0.05 \times 10^{-3}/M_{\pi^+}$, which is about 5%. The uncertainty of the neutron S-wave threshold amplitude is estimated to be the same. Consequently, our estimate of the error on the single nucleon amplitude is 5%.

We now switch to the two-nucleon contribution. In Coulomb gauge, only the two Feynman diagrams shown in Fig. 2 contribute at threshold at third order [5,6]. Their contribution to the multipoles

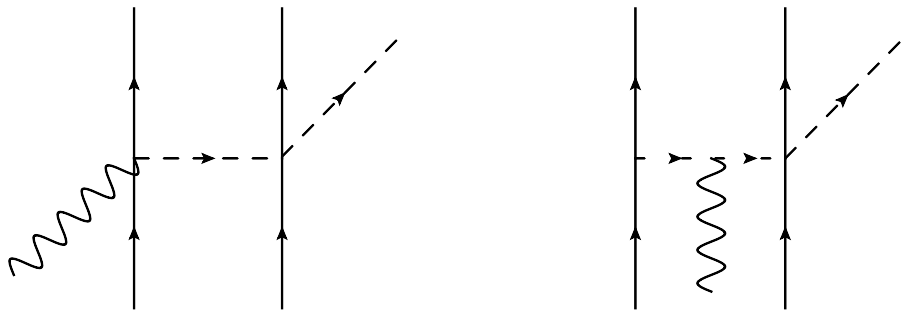

Figure 2: Leading two-nucleon contributions to the nuclear pion production matrix element at threshold. Solid, dashed and wiggly lines denote nucleons, pions and photons, in order.

can be written as

$$\begin{aligned} E_{0+}^{\rm 2N} &= K_{\rm 2N}\,(F_T^{(a)} - F_T^{(b)})\ , \\ L_{0+}^{\rm 2N} &= K_{\rm 2N}\,(F_L^{(a)} - F_L^{(b)})\ , \end{aligned} \tag{7}$$

with the prefactor

$$K_{\rm 2N} = \frac{M_\pi e g_A m_{\rm 3N}}{16\pi(m_{\rm 3N}+M_\pi)(2\pi)^3 F_\pi^3} \approx 0.135\ {\rm fm}\ \times 10^{-3}/M_{\pi^+}\ . \tag{8}$$

The numerical value for $K_{\rm 2N}$ was obtained using $g_A = 1.26$ for the axial-vector coupling constant, $F_\pi = 93$ MeV for the pion decay constant, and the neutral pion mass $M_\pi = 135$ MeV. Note that we use the older values for g_A and F_π to be consistent with the numbers used in the evaluation of the single nucleon multipoles [3, 4]. The transverse and longitudinal form factors $F_{T/L}^{(a)}$ and $F_{T/L}^{(b)}$ corresponding to diagrams (a) and (b), respectively, are

$$F_{T/L}^{(a)}\,\vec\epsilon_{\lambda,{\rm T/L}}\cdot\vec S_{M_J'M_J} = \frac{3}{2}\left\langle M_J'\left|\frac{\vec\epsilon_{\lambda,{\rm T/L}}\cdot(\vec\sigma_1+\vec\sigma_2)(\vec\tau_1\cdot\vec\tau_2-\tau_1^z\tau_2^z)}{\vec q\,'^2}\right|M_J\right\rangle_\psi\ , \tag{9}$$

and

$$F_{T/L}^{(b)}\,\vec\epsilon_{\lambda,{\rm T/L}}\cdot\vec S_{M_J'M_J} = 3\left\langle M_J'\left|\frac{(\vec\tau_1\cdot\vec\tau_2-\tau_1^z\tau_2^z)\left[(\vec q\,'-\vec k)\cdot(\vec\sigma_1+\vec\sigma_2)\right]\left[\vec\epsilon_{\lambda,{\rm T/L}}\cdot(\vec q\,'-\vec k/2)\right]}{\left[(\vec q\,'-\vec k)^2+M_{\pi^+}^2\right]\vec q\,'^2}\right|M_J\right\rangle_\psi\ , \tag{10}$$

where $\vec q\,' = \vec p_{12} - \vec p\,'_{12} + \vec k/2$ is the momentum of the exchanged pion and $\vec p_{12} = (\vec k_1 - \vec k_2)/2$, $\vec p\,'_{12} = (\vec k\,'_1 - \vec k\,'_2)/2$ are the initial and final Jacobi momenta of nucleons 1 and 2, respectively. The integral for the form factors $F_{T/L}^{(a)}$ contains an integrable singularity which can be removed by an appropriate variable transformation. Then, the form factors can be evaluated using Monte Carlo integration in the same way as the form factors for the single-nucleon contribution. Our results for $F_{T/L}^{(a)} - F_{T/L}^{(b)}$ are given in Table 2. The first error is again the theory error estimated from the cutoff variation in the chiral interaction as described above. The second error is the statistical error from the Monte Carlo integration which is about half the size of the theory error.

nucleus	^{3}He	^{3}H
$F_T^{(a)} - F_T^{(b)}$ [fm^{-1}]	$-29.3(2)(1)$	$-29.7(2)(1)$
$F_L^{(a)} - F_L^{(b)}$ [fm^{-1}]	$-22.9(2)(1)$	$-23.2(1)(1)$

Table 2: Numerical results for the form factors $F_{T/L}^{(a)} - F_{T/L}^{(b)}$ parameterizing two-body contributions in units of fm^{-1}. The first error is our estimation of the theoretical uncertainty resulting from the truncation of the chiral expansion while the second one is the statistical error from the Monte Carlo integration.

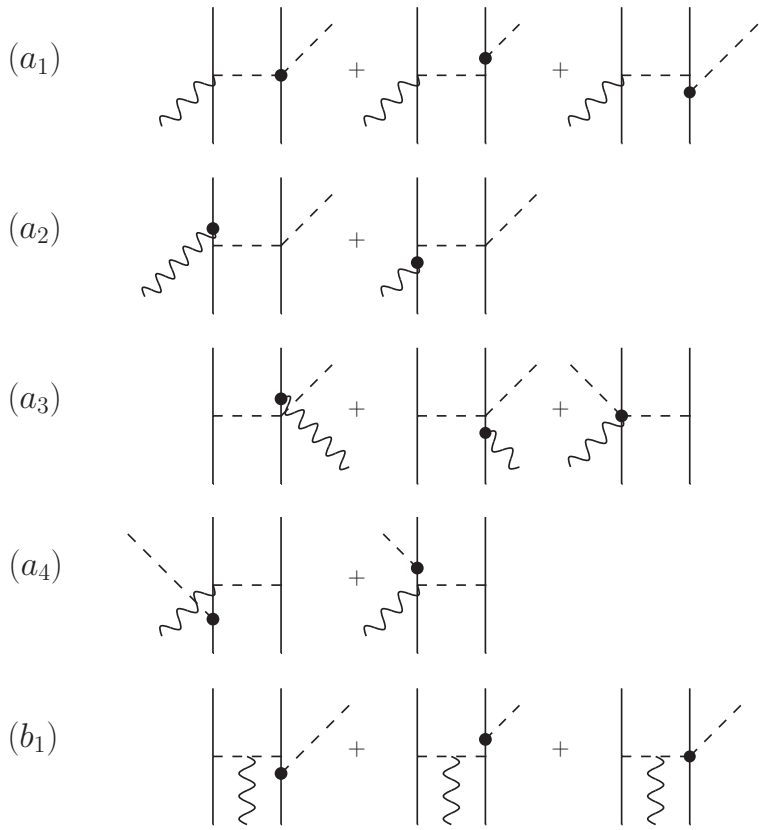

Figure 3: Subleading static two-nucleon contributions to the nuclear pion production matrix element at threshold. The filled circle denotes an insertion from the dimension two effective Lagrangian. For further notations, see Fig. 2.

2.3 Fourth order contributions

Apart from the fourth order corrections already included in the single nucleon multipoles E_{0+} and L_{0+}, there are various fourth order corrections that arise due to the presence of the other two nucleons in the tri-nucleon system considered here. First, there are the boost corrections that arise from the observation that within a nucleus the threshold for pion production is shifted compared to the free threshold. For light systems as considered here, this essentially induces P-wave contributions as detailed in Sec. 2.3.1. Second, there are further corrections to the two-nucleon production operator displayed in Figs. 3 and 4. These can be grouped in two categories, namely the so-called static and the

so-called recoil corrections. The static corrections are shown in Fig. 3. They involve - as the leading 2N corrections do - static propagators but one insertion from the dimension two chiral effective pion-nucleon Lagrangian. The recoil corrections feature corrections to the static propagators with only insertions from the leading order (dimension one) chiral Lagrangian. These corrections are most conveniently derived in time-ordered perturbation theory. The corresponding diagrams are shown in Fig. 4. The boxes indicate the regions where the two energy denominators whose $1/m_N$-expansion generates these corrections can appear (see Ref. [25] for more details). These two types of corrections will be discussed in Sec. 2.3.2 and Sec. 2.3.3, in order.

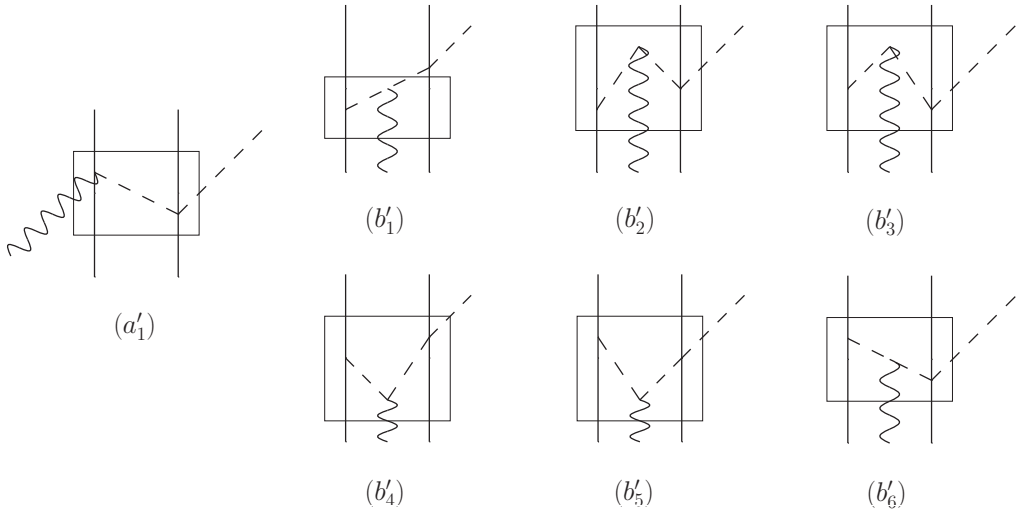

Figure 4: Subleading recoil two-nucleon contributions to the nuclear pion production matrix element at threshold in time-ordered perturbation theory. The boxes indicate the regions where the two energy denominators to be expanded can appear Further notation as in Fig. 2.

2.3.1 Boost corrections to the one-nucleon contributions

The proton and neutron production amplitudes are calculated in the (N,γ) center-of-mass system (cms). The boost of a $(3N,\gamma)$-cms four-vector p to the (N,γ)-cms four-vector p^* has the general form

$$\begin{pmatrix} p^{0*} \\ \vec{p}^{\,*} \end{pmatrix} = \begin{pmatrix} \gamma & -\gamma\vec{\beta} \\ -\gamma\vec{\beta} & (\mathbb{1}_3 - P_{\vec{\beta}}) + \gamma P_{\vec{\beta}} \end{pmatrix} \begin{pmatrix} p^0 \\ \vec{p} \end{pmatrix} = \begin{pmatrix} \gamma(p^0 - \vec{\beta}\cdot\vec{p}) \\ -\gamma\vec{\beta}p^0 + \vec{p}_\perp + \gamma\vec{p}_\parallel \end{pmatrix}, \tag{11}$$

where $P_{\vec{\beta}}$ is the projection operator onto the $\vec{\beta}$-direction, i.e. $P_{\vec{\beta}}\,\vec{x} = (\hat{\beta}\cdot\vec{x})\hat{\beta}$, $\vec{p}_\parallel = P_{\vec{\beta}}\,\vec{p}$ is the parallel part, and $\vec{p}_\perp = (1 - P_{\vec{\beta}})\vec{p}$ the perpendicular part of $\vec{p} = \vec{p}_\parallel + \vec{p}_\perp$ with respect to $\vec{\beta}$. To determine $\vec{\beta}$, we consider $\vec{k}_1 + \vec{k}$. In the (N,γ)-cms this combination has to vanish, i.e. $\vec{k}_1^{\,*} + \vec{k}^{\,*} = 0$. We have

$$\vec{k}_1^{\,*} + \vec{k}^{\,*} = \gamma\left(-\vec{\beta}(k_1^0 + k^0) + P_{\vec{\beta}}(\vec{k}_1 + \vec{k})\right) + (1 - P_{\vec{\beta}})(\vec{k}_1 + \vec{k}) \stackrel{!}{=} \vec{0}. \tag{12}$$

Because linearly independent (even orthogonal) vectors have to vanish separately, i.e.

$$\begin{aligned} (1 - P_{\vec{\beta}})(\vec{k}_1 + \vec{k}) &= \vec{0}\,, \\ -\vec{\beta}(k_1^0 + k^0) + P_{\vec{\beta}}(\vec{k}_1 + \vec{k}) &= \vec{0}\,, \end{aligned}$$

we conclude that

$$\vec{\beta} = \frac{\vec{k}_1 + \vec{k}}{k_1^0 + k^0} = \frac{\vec{k}_1' + \vec{q}}{k_1'^0 + q^0} = \frac{\vec{p}_{12}' - \vec{p}_3'/2 + 2\vec{q}/3}{\sqrt{(\vec{p}_{12}' - \vec{p}_3'/2 - \vec{q}/3)^2 + m_N^2} + q^0}. \tag{13}$$

For the definition of the Jacobi momenta used above, see Eqs. (9, 10). Near the static limit we have

$$\begin{aligned}\vec{\beta} &= \frac{\vec{p}_{12}' - \vec{p}_3'/2 + 2\vec{q}/3}{m_N} \left(\sqrt{\frac{(\vec{p}_{12}' - \vec{p}_3'/2 - \vec{q}/3)^2}{m_N^2} + 1} + \frac{\sqrt{\vec{q}^2 + M_\pi^2}}{m_N} \right)^{-1} \\ &= \frac{\vec{p}_{12}' - \vec{p}_3'/2 + 2\vec{q}/3}{m_N} + \mathcal{O}\left(m_N^{-2}\right) \xrightarrow{\text{threshold}} \frac{\vec{p}_{12}' - \vec{p}_3'/2}{m_N} + \mathcal{O}\left(m_N^{-2}\right), \end{aligned} \tag{14}$$

and thus $\gamma = \left(1 - \beta^2\right)^{-1/2} = 1 + \mathcal{O}\left(m_N^{-2}\right)$. Correspondingly, a general four-vector p^μ in the $(3N, \gamma)$-cms transforms to the (N, γ)-cms as

$$p^{0*} = \gamma(p^0 - \vec{\beta} \cdot \vec{p}) = p^0 - \frac{\vec{p}_{12}' - \vec{p}_3'/2 + 2\vec{q}/3}{m_N} \cdot \vec{p} \xrightarrow{\text{threshold}} p^0 - \frac{\vec{p}_{12}' - \vec{p}_3'/2}{m_N} \cdot \vec{p}, \tag{15}$$

$$\vec{p}^* = -\gamma\vec{\beta}p^0 + \vec{p}_\perp + \gamma\vec{p}_\parallel = \vec{p} - \frac{\vec{p}_{12}' - \vec{p}_3'/2 + 2\vec{q}/3}{m_N} p^0 \xrightarrow{\text{threshold}} \vec{p} - \frac{\vec{p}_{12}' - \vec{p}_3'/2}{m_N} p^0, \tag{16}$$

to first order in the inverse nucleon mass. At threshold, the boosted energy and momentum for the photon (k^{0*}, $\vec{k}^*$) and pion (q^{0*}, $\vec{q}^*$), as well as the time- and space-like components of the photon polarization vector (ϵ_λ^{0*}, $\vec{\epsilon}_\lambda^*$) are thus given by:

$$\begin{aligned} k^{0*} &= k^0 - \frac{(\vec{p}_{12}' - \vec{p}_3'/2) \cdot \vec{k}}{m_N}, & \vec{k}^* &= \vec{k} - \frac{k^0}{m_N}(\vec{p}_{12}' - \vec{p}_3'/2), \\ q^{0*} &= q^0 - \frac{(\vec{p}_{12}' - \vec{p}_3'/2) \cdot \vec{q}}{m_N} = M_\pi, & \vec{q}^* &= \vec{q} - \frac{q^0}{m_N}(\vec{p}_{12}' - \vec{p}_3'/2) = -\frac{M_\pi}{m_N}(\vec{p}_{12}' - \vec{p}_3'/2), \\ \epsilon_\lambda^{0*} &= \epsilon_\lambda^0 - \frac{(\vec{p}_{12}' - \vec{p}_3'/2) \cdot \vec{\epsilon}_\lambda}{m_N}, & \vec{\epsilon}_\lambda^* &= \vec{\epsilon}_\lambda - \frac{\epsilon_\lambda^0}{m_N}(\vec{p}_{12}' - \vec{p}_3'/2) = \vec{\epsilon}_\lambda. \end{aligned} \tag{17}$$

Since $\epsilon_\lambda^0 = 0$, the polarization vector does not change except for the time component.

To adopt the results for pion production off nucleons which were calculated in the (N, γ)-cms for our calculation on the tri-nucleon, the pion momentum in the $(3N, \gamma)$-cms at threshold, $\vec{q} = \vec{0}$, is boosted to the (N, γ)-cms value $\vec{q}^* = -(M_\pi/m_N)(\vec{p}_{12}' - \vec{p}_3'/2) =: -\mu(\vec{p}_{12}' - \vec{p}_3'/2)$ above threshold. The corresponding P-wave contribution reads (using the notation from Ref. [26])

$$\begin{aligned} \mathcal{M}_\lambda &= 2i(\vec{\epsilon}_\lambda \cdot \vec{S})(\hat{q}^* \cdot \hat{k})P_1 + 2i(\vec{\epsilon}_\lambda \cdot \hat{q}^*)(\hat{k} \cdot \vec{S})P_2 + (\vec{\epsilon}_\lambda \cdot [\hat{q}^* \times \hat{k}])P_3 \\ &\quad + 2i(\vec{\epsilon}_\lambda \cdot \hat{k})(\hat{k} \cdot \vec{S})(\hat{q}^* \cdot \hat{k})(P_4 - P_5 - P_1 - P_2) + 2i(\vec{\epsilon}_\lambda \cdot \hat{k})(\hat{q}^* \cdot \vec{S})P_5 \\ &=: 2i(\vec{\epsilon}_{\lambda,\mathrm{T}} \cdot \vec{S})(\hat{q}^* \cdot \hat{k})P_1 + 2i(\vec{\epsilon}_{\lambda,\mathrm{T}} \cdot \hat{q}^*)(\hat{k} \cdot \vec{S})P_2 + (\vec{\epsilon}_{\lambda,\mathrm{T}} \cdot [\hat{q}^* \times \hat{k}])P_3 \\ &\quad + 2i(\vec{\epsilon}_{\lambda,\mathrm{L}} \cdot \vec{S})(\hat{q}^* \cdot \hat{k})P_4 + 2i(\vec{\epsilon}_{\lambda,\mathrm{L}} \cdot \hat{k})(\hat{q}_\mathrm{T}^* \cdot \vec{S})P_5. \end{aligned}$$

Close to threshold, the P-wave multipoles P_i behave as $P_i \approx \bar{P}_i|\vec{q}^{\,*}| = \mu\bar{P}_i|\vec{p}_{12}' - \vec{p}_3'/2|$ with

$$\begin{aligned} \bar{P}_1^p &= +0.0187 \text{ fm}^2\,, \quad \bar{P}_3^p = +0.0240 \text{ fm}^2\,, \quad \bar{P}_4^p = +0.0013 \text{ fm}^2\,, \\ \bar{P}_1^n &= +0.0134 \text{ fm}^2\,, \quad \bar{P}_3^n = +0.0234 \text{ fm}^2\,, \quad \bar{P}_4^n = +0.0003 \text{ fm}^2\,, \end{aligned} \tag{18}$$

where the numerical values refer to the P-wave low-energy theorems for pion photo- [3] and electroproduction [27]. Corrections to these theorems are beyond the accuracy of our calculation.

nucleus	^{3}He	^{3}H
F_1^{S+V}	$+0.004(3)(1)$	$+0.339(6)(1)$
F_1^{S-V}	$+0.338(5)(1)$	$+0.002(3)(1)$
F_3^{S+V}	$-0.015(2)(0)$	$-0.011(2)(0)$
F_3^{S-V}	$-0.011(2)(0)$	$-0.015(2)(0)$
F_4^{S+V}	$-0.019(5)(4)$	$+0.339(6)(4)$
F_4^{S-V}	$+0.337(6)(4)$	$-0.021(3)(4)$

Table 3: Numerical results for the boost correction form factors $F_i^{S\pm V}$ in units of [fm^{-1}]. The first error is our estimation of the theoretical uncertainty resulting from the truncation of the chiral expansion while the second one is the statistical error from the Monte Carlo integration.

In analogy to the S-wave case discussed above, we define the corresponding P-wave form factors

$$\begin{aligned}
\left(\vec{\epsilon}_{\lambda,\mathrm{T}}\cdot\vec{S}_{M'_J M_J}\right) F_1^{S/V} &= \left\langle M_{J'}\left| 3\left(\vec{\epsilon}_{\lambda,\mathrm{T}}\cdot\vec{S}_1\right)\left((\vec{p}\,'_{12}-\vec{p}\,'_3/2)\cdot\hat{k}\right) X^{S/V}\right| M_J\right\rangle_\psi ,\\
\left(\vec{\epsilon}_{\lambda,\mathrm{T}}\cdot\vec{S}_{M'_J M_J}\right) F_2^{S/V} &= \left\langle M_{J'}\left| 3\Big(\vec{\epsilon}_{\lambda,\mathrm{T}}\cdot(\vec{p}\,'_{12}-\vec{p}\,'_3/2)\Big)\left(\hat{k}\cdot\vec{S}_1\right) X^{S/V}\right| M_J\right\rangle_\psi ,\\
\left(\vec{\epsilon}_{\lambda,\mathrm{T}}\cdot\vec{S}_{M'_J M_J}\right) F_3^{S/V} &= \left\langle M_{J'}\left| -\frac{3}{2}i\left(\vec{\epsilon}_{\lambda,\mathrm{T}}\cdot[(\vec{p}\,'_{12}-\vec{p}\,'_3/2)\times\hat{k}]\right) X^{S/V}\right| M_J\right\rangle_\psi ,\\
\left(\vec{\epsilon}_{\lambda,\mathrm{L}}\cdot\vec{S}_{M'_J M_J}\right) F_4^{S/V} &= \left\langle M_{J'}\left| 3\left(\vec{\epsilon}_{\lambda,\mathrm{L}}\cdot\vec{S}_1\right)\left((\vec{p}\,'_{12}-\vec{p}\,'_3/2)\cdot\hat{k}\right) X^{S/V}\right| M_J\right\rangle_\psi ,\\
\left(\vec{\epsilon}_{\lambda,\mathrm{L}}\cdot\vec{S}_{M'_J M_J}\right) F_5^{S/V} &= \left\langle M_{J'}\left| 3\left(\vec{\epsilon}_{\lambda,\mathrm{L}}\cdot\hat{k}\right)\left((\hat{p}\,'_{12}-\vec{p}\,'_3/2)_{\mathrm{T}}\cdot\vec{S}_1\right) X^{S/V}\right| M_J\right\rangle_\psi ,
\end{aligned} \tag{19}$$

where the spin and isospin operators refer to nucleon 1. Further, we have introduced the notation $X^S = 1$, $X^V = \tau_1^z$. The contributions from the other nucleons are accounted for by the overall factor of three.

In terms of these form factors, the P-wave contribution to the 3N-production amplitude takes the form:

$$E_{0+}^{1N,\mathrm{boost}} \approx -0.546\mu \sum_{i=1}^{3}\left(F_i^{S+V}\,\bar{P}_i^p + F_i^{S-V}\,\bar{P}_i^n\right) , \tag{20}$$

$$L_{0+}^{1N,\mathrm{boost}} \approx -0.546\mu \sum_{i=4}^{5}\left(F_i^{S+V}\,\bar{P}_i^p + F_i^{S-V}\,\bar{P}_i^n\right) , \tag{21}$$

where $F_i^{S\pm V} = F_i^S \pm F_i^V$. These form factors are evaluated using the same Monte Carlo method as employed for the S-waves. The numerical values are collected in Tab. 3. Note that F_2 and F_5 come out to be consistent with zero and therefore not listed in the table. As before, the proton contribution is dominant in ^{3}H, whereas the neutron one features prominently in ^{3}He.

Notice that in contrast to the single-nucleon corrections, we do not need to employ a special treatment for boost corrections to the leading two-nucleon contributions. All $1/m_N$-corrections to the leading three-body contributions to the production operator needed in the calculations are treated on the same footing as described in section 2.3.3.

2.3.2 Fourth order two-nucleon contributions

Similar to the leading order graphs displayed in Fig. 2, one has additional contributions at NNLO, which are displayed as diagram classes a_1, a_2, a_3, a_4, and b_1 in Fig. 3. These involve the insertion of one dimension-two operator from the chiral effective Lagrangian. As in the case of the deuteron, only the operators $\sim 1/2m_N$, $\sim g_A/2m_N$ or $\sim \kappa_{p,n}$ contribute, while all contributions proportional to the LECs c_i vanish at threshold. All these Feynman diagrams give corrections of the form $iT_{12} = \mathcal{N}\hat{\mathcal{O}}_{12}$ and involve multiples of the generic prefactor $\mathcal{N} = (eg_A m_N)/(2F_\pi^3)$. They lead to contributions of the form

$$\mathcal{M} = 2iK_{2N}^{q^4} \left\langle \hat{\mathcal{O}}_{12} + \hat{\mathcal{O}}_{21} \right\rangle_\Psi \tag{22}$$

with

$$K_{2N}^{q^4} = -\frac{1}{2}\frac{m_{3N}}{m_N}\frac{1}{8\pi(m_{3N}+M_\pi)}\frac{\mathcal{N}}{(2\pi)^3 2m_N} = -K_{2N}\frac{1}{4m_N M_\pi} \approx -0.0104\,\mathrm{fm}^3\frac{10^{-3}}{M_{\pi^+}} \tag{23}$$

to account for the phase space and normalization. The prefactor of the 2N contributions at order q^4, $K_{2N}^{q^4}$ is suppressed considerably compared to the corresponding prefactor at order q^3, K_{2N}. This has to be kept in mind when we discuss the numerical results for the fourth order corrections.

We are now in a position to evaluate the various classes of diagrams, following the calculations for the deuteron from Refs. [7, 25]. The corrections to diagram (a) in Fig. 2 which are given in Fig. 3(a_1)-(a_4) read

$$\begin{aligned}
iT_{12}^{NN,a_1} &= (1-2g_A^2)\frac{em_N g_A}{2F_\pi^3}\frac{\vec{\epsilon}_{\lambda,\mathrm{T}}\cdot\vec{\sigma}_1}{\vec{q}\,'^2}(\vec{\tau}_1\cdot\vec{\tau}_2 - \tau_1^z\tau_2^z)\,\left(\vec{q}\,'\cdot\vec{q}\,' + 2\vec{q}\,'\cdot\vec{p}\,'_{12}\right)\,, \\
iT_{12}^{NN,a_2} &= \frac{em_N g_A}{F_\pi^3}\frac{\vec{\epsilon}_{\lambda,\mathrm{T}}\cdot\left((\vec{q}\,' + 2\vec{p}\,'_{12} - \vec{k})\,\vec{\sigma}_1\cdot\vec{q}\,' + i[\vec{q}\,'\times\vec{k}](1+\kappa_V)\right)}{\vec{q}\,'^2}(\vec{\tau}_1\cdot\vec{\tau}_2 - \tau_1^z\tau_2^z)\,, \\
iT_{12}^{NN,a_3} &= \frac{em_N g_A}{F_\pi^3}\frac{\vec{\epsilon}_{\lambda,\mathrm{T}}\cdot\left(\vec{q}\,' + 2\vec{p}\,'_{12} - \vec{k} + i[\vec{\sigma}_1\times\vec{k}](1+\kappa_V)\right)\vec{\sigma}_2\cdot\vec{q}\,'}{\vec{q}\,'^2 + M_{\pi^+}^2}(\vec{\tau}_1\cdot\vec{\tau}_2 - \tau_1^z\tau_2^z)\,, \\
iT_{12}^{NN,a_4} &= g_A^2\frac{em_N g_A}{F_\pi^3}\frac{\vec{\epsilon}_{\lambda,\mathrm{T}}\cdot\left(-(\vec{q}\,' + 2\vec{p}\,'_{12} - \vec{k}) + i[\vec{\sigma}_1\times(\vec{q}\,' - \vec{k})]\right)\vec{\sigma}_2\cdot\vec{q}\,'}{\vec{q}\,'^2 + M_{\pi^+}^2}(\vec{\tau}_1\cdot\vec{\tau}_2 - \tau_1^z\tau_2^z)\,.
\end{aligned} \tag{24}$$

The corrections to diagram (b) in Fig. 2 which are given in Fig. 3(b_1) read

$$iT_{12}^{NN,b_1} = -\left(1-2g_A^2\right)\frac{em_N g_A}{2F_\pi^3}\frac{\vec{\sigma}_1\cdot\vec{q}\,''\,\vec{\epsilon}_{\lambda,\mathrm{T}}\cdot(\vec{q}\,'' + \vec{q}\,')}{\left(\vec{q}\,''\cdot\vec{q}\,'' + M_{\pi^+}^2\right)(\vec{q}\,'\cdot\vec{q}\,')}(\vec{\tau}_1\cdot\vec{\tau}_2 - \tau_1^z\tau_2^z)\,\left(\vec{q}\,'\cdot\vec{q}\,' + 2\vec{q}\,'\cdot\vec{p}\,'_{12}\right). \tag{25}$$

with $\vec{q}\,'$ as before and $\vec{q}\,'' = \vec{q}\,' - \vec{k}$.

2.3.3 $1/m_N$-corrections to leading two-nucleon contributions

Furthermore, there are $1/m_N$-corrections to leading two-nucleon diagrams some of which are shown in Fig. 2. They have been worked out within the Q-box framework in Ref. [25]. The corresponding diagrams a_1', b_1', b_2', b_3', b_4', b_5', and b_6' are displayed in Fig. 4. The boxes indicate the regions where the two energy denominators whose $1/m_N$-expansion generates the corrections can appear (see Ref. [25] for more details).

For the expressions of the various diagrams, we use the following abbreviations:

$$\omega' = \sqrt{\vec{q}\,'^2 + M_{\pi^+}^2} \quad \text{and} \quad \omega'' = \sqrt{\vec{q}\,''^2 + M_{\pi^+}^2} \ . \tag{26}$$

With that, the correction to diagram (a) in Fig. 2 which are given in Fig. 4(a_1') read

$$iT_{12}^{NN,a_1'} = \frac{em_N g_A}{8F_\pi^3} \frac{\vec{\epsilon}_{\lambda,\mathrm{T}} \cdot \vec{\sigma}_1 (\omega' - M_\pi)}{\omega'(\omega' + M_\pi)^2} \vec{k} \cdot (-2\vec{q}\,' - 2\vec{p}\,'_{12} + \vec{k})(\vec{\tau}_1 \cdot \vec{\tau}_2 - \tau_1^z \tau_2^z) \ , \tag{27}$$

whereas the various corrections to diagram (b) in Fig. 2 which are given in Fig. 4(b_1')-(b_6') take the form

$$\begin{aligned} iT_{12}^{NN,b_1'} &= \frac{em_N g_A}{16F_\pi^3} \frac{\vec{\sigma}_1 \cdot \vec{q}\,'' \vec{\epsilon}_{\lambda,\mathrm{T}} \cdot (\vec{q}\,'' + \vec{q}\,')(\omega' + M_\pi)}{\omega' \omega''^3} (\vec{\tau}_1 \cdot \vec{\tau}_2 - \tau_1^z \tau_2^z) \\ &\quad \times \left(\frac{-\vec{q}\,' \cdot \vec{q}\,' - \vec{q}\,' \cdot \vec{p}\,'_{12} + 2(\vec{q}\,' + \vec{p}\,'_{12}) \cdot \vec{k} - \vec{k}^2}{\omega' - M_\pi} + \frac{\vec{q}\,' \cdot \vec{q}\,' + \vec{q}\,' \cdot \vec{p}\,'_{12}}{\omega' - \omega'' - M_\pi} \right) \ , \end{aligned}$$

$$\begin{aligned} iT_{12}^{NN,b_2'} &= \frac{em_N g_A}{16F_\pi^3} \frac{\vec{\sigma}_1 \cdot \vec{q}\,'' \vec{\epsilon}_{\lambda,\mathrm{T}} \cdot (\vec{q}\,'' + \vec{q}\,')(\omega' - M_\pi)}{\omega' \omega''^3 (\omega' + \omega'' + M_\pi)^2} (\vec{\tau}_1 \cdot \vec{\tau}_2 - \tau_1^z \tau_2^z) \\ &\quad \times \left(2\omega'' \left\{ \vec{q}\,' \cdot \vec{q}\,' + \vec{q}\,' \cdot \vec{p}\,'_{12} - 2(\vec{q}\,' + \vec{p}\,'_{12}) \cdot \vec{k} + \vec{k}^2 \right\} + (\omega' + M_\pi) \left\{ -2(\vec{q}\,' + \vec{p}\,'_{12}) \cdot \vec{k} + \vec{k}^2 \right\} \right) \ , \\ iT_{12}^{NN,b_3'} &= \frac{em_N g_A}{16F_\pi^3} \frac{\vec{\sigma}_1 \cdot \vec{q}\,'' \vec{\epsilon}_{\lambda,\mathrm{T}} \cdot (\vec{q}\,'' + \vec{q}\,')(\omega' - M_\pi)}{\omega' \omega''^3 (\omega' + \omega'' + M_\pi)^2 (\omega' + \omega'')^2} (\vec{\tau}_1 \cdot \vec{\tau}_2 - \tau_1^z \tau_2^z) \\ &\quad \times \left(\omega'' \left\{ 2(\vec{q}\,' + \vec{p}\,'_{12}) \cdot \vec{k} - \vec{k}^2 \right\} + 2(\omega' + M_\pi) \left\{ \vec{q}\,' \cdot \vec{q}\,' + \vec{q}\,' \cdot \vec{p}\,'_{12} \right\} \right) \ , \\ iT_{12}^{NN,b_4'} &= \frac{em_N g_A}{16F_\pi^3} \frac{\vec{\sigma}_1 \cdot \vec{q}\,'' \vec{\epsilon}_{\lambda,\mathrm{T}} \cdot (\vec{q}\,'' + \vec{q}\,')(\omega' + M_\pi)}{\omega' \omega''^3 (\omega' + \omega'' + M_\pi)^2 (\omega' + \omega'')^2} (\vec{\tau}_1 \cdot \vec{\tau}_2 - \tau_1^z \tau_2^z) \\ &\quad \times \left(\omega'' \left\{ \vec{q}\,' \cdot \vec{q}\,' + \vec{q}\,' \cdot \vec{p}\,'_{12} - 2(\vec{q}\,' + \vec{p}\,'_{12}) \cdot \vec{k} + \vec{k}^2 \right\} - (\omega' - M_\pi) \left\{ \vec{q}\,' \cdot \vec{q}\,' + \vec{q}\,' \cdot \vec{p}\,'_{12} \right\} \right) \ , \\ iT_{12}^{NN,b_5'} &= \frac{em_N g_A}{16F_\pi^3} \frac{\vec{\sigma}_1 \cdot \vec{q}\,'' \vec{\epsilon}_{\lambda,\mathrm{T}} \cdot (\vec{q}\,'' + \vec{q}\,')(\omega' + M_\pi)}{\omega' \omega''^3 (\omega' + \omega'' - M_\pi)^2} (\vec{\tau}_1 \cdot \vec{\tau}_2 - \tau_1^z \tau_2^z) \\ &\quad \times \left(2\omega'' \left\{ \vec{q}\,' \cdot \vec{q}\,' + \vec{q}\,' \cdot \vec{p}\,'_{12} - 2(\vec{q}\,' + \vec{p}\,'_{12}) \cdot \vec{k} + \vec{k}^2 \right\} + (\omega' - M_\pi) \left\{ -2(\vec{q}\,' + \vec{p}\,'_{12}) \cdot \vec{k} + \vec{k}^2 \right\} \right) \ , \\ iT_{12}^{NN,b_6'} &= \frac{em_N g_A}{16F_\pi^3} \frac{\vec{\sigma}_1 \cdot \vec{q}\,'' \vec{\epsilon}_{\lambda,\mathrm{T}} \cdot (\vec{q}\,'' + \vec{q}\,')(\omega' - M_\pi)}{\omega' \omega''^3 (\omega' + M_\pi)^2} (\vec{\tau}_1 \cdot \vec{\tau}_2 - \tau_1^z \tau_2^z) \\ &\quad \times \left((\omega' + \omega'' + M_\pi) \left\{ 2(\vec{q}\,' + \vec{p}\,'_{12}) \cdot \vec{k} - \vec{k}^2 \right\} \right) . \end{aligned} \tag{28}$$

3 Results and discussion

We are now in a position to evaluate the nuclear S-wave multipoles. They are given as the sum of the one- and two-nucleon contributions given in the previous section,

$$E_{0+} = E_{0+}^{\mathrm{1N}} + E_{0+}^{\mathrm{2N}} \ , \quad L_{0+} = L_{0+}^{\mathrm{1N}} + L_{0+}^{\mathrm{2N}} \ . \tag{29}$$

Combining the leading and subleading corrections to the two-nucleon production operators discussed above with the subleading chiral perturbation theory results for the single-nucleon multipoles at $\mathcal{O}(p^4)$ [3, 4, 28]

$$\begin{aligned} E_{0+}^{\pi^0 p} &= -1.16 \times 10^{-3}/M_{\pi^+} \ , \quad E_{0+}^{\pi^0 n} = +2.13 \times 10^{-3}/M_{\pi^+} \ , \\ L_{0+}^{\pi^0 p} &= -1.35 \times 10^{-3}/M_{\pi^+} \ , \quad L_{0+}^{\pi^0 n} = -2.41 \times 10^{-3}/M_{\pi^+} \ , \end{aligned} \tag{30}$$

^{3}He	1N (q^4)	2N (q^3)	1N-boost	2N-static (q^4)	2N-recoil (q^4)	total
E_{0+} $[10^{-3}/M_{\pi^+}]$	$+1.71(4)(9)$	$-3.95(3)$	$-0.23(1)$	$-0.02(0)(1)$	$+0.01(2)(1)$	$-2.48(11)$
L_{0+} $[10^{-3}/M_{\pi^+}]$	$-1.89(4)(9)$	$-3.09(2)$	$-0.00(0)$	$-0.07(1)(1)$	$+0.07(7)(0)$	$-4.98(12)$
^{3}H	1N (q^4)	2N (q^3)	1N-boost	2N-static (q^4)	2N-recoil (q^4)	total
E_{0+} $[10^{-3}/M_{\pi^+}]$	$-0.93(3)(5)$	$-4.01(3)$	$-0.35(1)$	$-0.02(1)(1)$	$+0.01(2)(0)$	$-5.28(7)$
L_{0+} $[10^{-3}/M_{\pi^+}]$	$-0.99(4)(5)$	$-3.13(1)$	$-0.02(0)$	$-0.07(0)(1)$	$+0.07(7)(0)$	$-4.14(10)$

Table 4: Numerical results for the 3N multipoles. The first error is our estimation of the theoretical uncertainty resulting from the truncation of the chiral expansion while the second one is the statistical error from the Monte Carlo integration (with the exception of the $1N$ contributions as explained in the text). For the total result only the combined error is given.

we obtain for the threshold multipoles on ^{3}He and on ^{3}H the values listed in Table 4. For $E_{0+}^{\pi^0 p}$ we took an average of Refs. [4, 28]. The neutron amplitude uses the updated LECs from [4] based on the formalism from [4] but is not explicitely given in that paper. Note that the values for the single nucleon multipoles in Eq. (30) are consistent with the unpolarized data of [29] and a recent calculation in the chiral unitary approach [30]. The extractions of the proton S-wave photoproduction multipoles based on CHPT using various approximations show a 5% uncertainty [24]. Consequently, we assign a 5% error to the single-nucleon multipoles.[#6]

We remark that in the heavy baryon calculations of Refs. [3,4], the physical pion masses have been used in the kinematics. Moreover, the physical pion masses were used in evaluating the corresponding loop diagrams. Thus the production as well as the second threshold due to the $\pi^+ n$ intermediate state are correctly accounted for. The same approach is used here. Therefore, the multipole values in Eq. (30) can indeed be tested in pion production off the tri-nucleon.

In Table 4, adding the first two columns gives the leading one-loop result from Ref. [10]. The fourth order corrections are given separately for the boost of the single nucleon terms (third column) as well as the contributions described in sections 2.3.2 and 2.3.3 and referred to as static and recoil, respectively. The complete one-loop result can be found in the sixth column. The first error given is an estimate of the theory error from higher orders in chiral EFT, the second error is the statistical error from the Monte Carlo integration. Notice that the statistical error is negligible compared to theory error. The 5% error from the single-nucleon amplitudes discussed above is not included in the numbers for the theory error, but appears as the second error of the single nucleon contribution in the table. For the total result only the combined error is given. Overall, we find that these fourth order corrections for the electric dipole amplitude E_{0+} for both tri-nuclear systems come out to be very small, much smaller than in case of the deuteron. This can be, in part, traced back to the smaller values of the various form factors (for the boost corrections) and also to the small prefactor K_{2N}^{q4}, cf. Eq. (23), for the two-nucleon contributions. For the longitudinal amplitude L_{0+}, the sum of the fourth order corrections is consistent with zero within the uncertainties. This can be understood as follows: First, the boost corrections are proportional to the P-wave multipole P_4, which is much smaller than the corresponding multipoles P_1, P_3 that appear in the electric dipole amplitude, cf. Eq. (18). Second, there are almost perfect cancellations between the static and the recoil contributions for both tri-nucleon systems. These cancellations are accidental in the sense that they can not be traced back to any symmetry or

[#6] We note that it is misleading to estimate the theory uncertainty from comparing third and fourth order results due to the abnormally large contribution of the triangle diagram. The theory uncertainty has therefore been estimated from a comparison of fitting various data sets available and using variations of the ChPT amplitude that account for unitarity exactly.

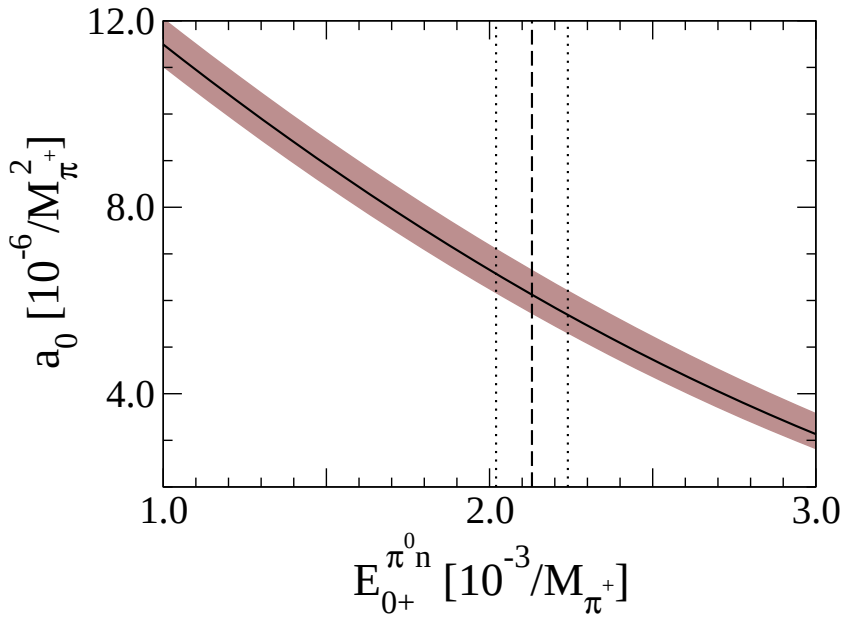

Figure 5: Sensitivity of a_0 for ^{3}He in units of $10^{-6}/M_{\pi^+}^2$ to the single-neutron multipole $E_{0+}^{\pi^0 n}$ in units of $10^{-3}/M_{\pi^+}$. The vertical dashed line gives the CHPT prediction for $E_{0+}^{\pi^0 n}$ and the vertical dotted lines indicate the 5% error in the prediction. The shaded band indicates the theory error estimated from the cutoff variation and a 5% error in $E_{0+}^{\pi^0 p}$ as described in the text.

small prefactor. In summary, we find that the chiral expansion for the S-wave multipoles at threshold converges fast and that the largest uncertainty remains in the single nucleon production amplitudes. We also remark that the fourth order corrections to the electric dipole amplitudes of the tri-nucleon systems are sizably smaller than for the deuteron.

Now, let us concentrate on photoproduction. The threshold S-wave cross section for pion photoproduction a_0 is given by

$$a_0 = \left.\frac{|\vec{k}\,|}{|\vec{q}\,|}\frac{d\sigma}{d\Omega}\right|_{\vec{q}=0} = |E_{0+}|^2 \ . \tag{31}$$

In Fig. 5, we illustrate the sensitivity of a_0 to the single-neutron multipole $E_{0+}^{\pi^0 n}$. The shaded band indicates the theory error estimated from the cutoff variation as described above and a 5% error in $E_{0+}^{\pi^0 p}$. As shown above, the uncertainties related to the nuclear effects are of the order of one percent, i.e. completely negligible. So our estimate of a 10% uncertainty of the 2N contributions in Ref. [10] driven by the analogy to the deuteron case [6] turns out to be much too conservative. The vertical dashed line indicates the CHPT prediction $E_{0+}^{\pi^0 n} = 2.13 \times 10^{-3}/M_{\pi^+}$. Changing this value by $\pm 20\%$ leads to changes in a_0 of about $\pm 30\%$. Thus, the ^{3}He nucleus is a very promising target to test the CHPT prediction for $E_{0+}^{\pi^0 n}$. On the contrary, neutral pion production on ^{3}H is rather insensitive to $E_{0+}^{\pi^0 n}$: a variation of $E_{0+}^{\pi^0 n}$ in the range $0 \ldots 3$ (in units of $10^{-3}/M_{\pi^+}$) changes a_0 only by 1%.

Next we compare our predictions with the available data. The consistency of the CHPT prediction for the single-neutron multipole with the measured S-wave threshold amplitude on the deuteron from Saclay and Saskatoon is well established, see Refs. [2, 6]. The reanalyzed measurement of the S-wave amplitude for ^{3}He at Saclay gives $E_3 = (-3.5 \pm 0.3) \times 10^{-3}/M_{\pi^+}$ [11, 12], which is related to a_0

according to

$$|E_{0+}|^2 = |E_3|^2 \left| \frac{F_T^{S-V}}{2} \right|^2 \left(\frac{1 + M_\pi/m_N}{1 + M_\pi/3m_N} \right)^2 \ . \tag{32}$$

Here, we have approximated the $A = 3$ body form factor $\mathcal{F}_A$ of Argan et al. [12] by the numerically dominant form factor F_T^{S-V} for ^{3}He, cf. Tab. 1. This results in

$$E_{0+} = (-2.8 \pm 0.2) \times 10^{-3}/M_{\pi^+} \ , \tag{33}$$

assuming the same sign as for our ^{3}He prediction in Table 4. In magnitude, the extracted value is about 25% above the leading one-loop prediction $E_{0+} = -2.24(11) \times 10^{-3}/M_{\pi^+}$. The discrepancy is reduced for the fourth order result $E_{0+} = -2.48(11) \times 10^{-3}/M_{\pi^+}$, which is about 12% below the experimental value in Eq. (33). Taking into account the errors, our fourth order result is consistent with the experiment of Argan et al. [12]. Given the model-dependence that is inherent to the analysis of Ref. [12], it is obvious that a more precise measurement using CW beams and modern detectors is very much called for. Our calculation establishes a model independent connection between the trinucleon multipole measured in such an experiment and the single neutron multipole to be extracted.

4 Summary and outlook

In this paper, we have presented a calculation of the subleading two-nucleon operators for threshold neutral pion photo- and electroproduction off the tri-nucleon systems ^{3}H and ^{3}He. This completes the one-loop calculation at order $\mathcal{O}(q^4)$ in the standard heavy baryon counting. The single nucleon contributions to that order and the leading third order two-nucleon contributions were already evaluated in the corresponding letter [10]. The production operator was evaluated in the framework of chiral nuclear effective field theory, in line with the earlier calculations for production off the deuteron [5–7]. To this order, it gets both one- and two-body contributions. Here, we have given explicit expressions for the fourth order two-nucleon contributions stemming from boost corrections for pion production off a single nucleon (such contributions only arise from the fact that in a nucleus the threshold for pion production is lowered as compared to the nucleon case), from static 2N contributions with one insertion from the dimension two chiral pion-nucleon Lagrangian and from recoil corrections to the pion- and nucleon propagators. We used the chiral wave functions of Refs. [17, 18] to calculate the S-wave 3N multipoles E_{0+} and L_{0+}. These wave functions are consistent with the pion production operator.

We have shown that all corrections at fourth order in the standard heavy baryon counting are very small, a few percent for the tri-nucleon electric dipole amplitudes and essentially vanishing for the corresponding longitudinal amplitudes. This suppression can be explained by very small boost correction and an accidental cancellation between the static and the recoil contibutions. We remark that these corrections are sizably smaller than in the deuteron case [6]. However, we note that the the role of nucleon recoil, accounting for the new scale $\chi = \sqrt{M_\pi m_N} \simeq 340$ MeV, needs to be investigated in more detail in view of the findings of Refs. [31, 32].

The theoretical uncertainty associated with the cutoff variation in the employed wave functions appears to be small (of the order of 3%). The dominant theoretical error at this order stems from the threshold pion production amplitude off the proton and the neutron, which is estimated to be about 5%. Consequently, we have explored the possibility to extract the elementary neutron multipole $E_{0+}^{\pi^0 n}$ from a neutral pion photoproduction measurement off ^{3}He. We found indeed a large sensitivity of the E_{0+} amplitude to $E_{0+}^{\pi^0 n}$. Given the very small uncertainty of the nuclear corrections as shown here, ^{3}He appears to be a promising target to test the counterintuitive CHPT prediction for $E_{0+}^{\pi^0 n}$ [3, 4].

We have also shown that our prediction for the ^{3}He S-wave multipole E_{0+} is roughly consistent with the value deduced from the old Saclay measurement of the threshold cross section [12]. A new measurement using modern technology and better methods to deal with few-body dynamics is urgently called for. The rapid energy dependence of $E_{0+}^{\pi^0 n}$ due to the close by charged pion production threshold presents a challenge for its experimental extraction. An calculation of pion production above threshold would be valuable in this context.

There are many other natural extensions of this work. They include investigating higher orders, the extension to virtual photons and pion electroproduction, production of charged pions, and considering heavier nuclear targets such as ^{4}He. Further work in these directions is in progress.

Acknowledgements

We thank Andreas Nogga for providing us with the chiral 3N wave functions and Hermann Krebs for discussions. Financial support by the Deutsche Forschungsgemeinschaft (SFB/TR 16, "Subnuclear Structure of Matter"), by the European Community Research Infrastructure Integrating Activity "Study of Strongly Interacting Matter" (acronym HadronPhysics3, Grant Agreement n. 283286) under the 7th Framework Programme of the EU and by the European Research Council (acronym NuclearEFT, ERC-2010-StG 259218) is gratefully acknowledged.

References

[1] D. R. Phillips, J. Phys. G **36** (2009) 104004 [arXiv:0903.4439 [nucl-th]].

[2] V. Bernard, Prog. Part. Nucl. Phys. **60** (2008) 82 [arXiv:0706.0312 [hep-ph]].

[3] V. Bernard, N. Kaiser and U.-G. Meißner, Z. Phys. C **70** (1996) 483 [arXiv:hep-ph/9411287].

[4] V. Bernard, N. Kaiser and U.-G. Meißner, Eur. Phys. J. A **11** (2001) 209 [arXiv:hep-ph/0102066].

[5] S. R. Beane, C. Y. Lee and U. van Kolck, Phys. Rev. C **52** (1995) 2914 [arXiv:nucl-th/9506017].

[6] S. R. Beane, V. Bernard, T.-S. H. Lee, U.-G. Meißner and U. van Kolck, Nucl. Phys. A **618** (1997) 381 [arXiv:hep-ph/9702226].

[7] H. Krebs, V. Bernard and U.-G. Meißner, Eur. Phys. J. A **22** (2004) 503 [arXiv:nucl-th/0405006].

[8] E. Epelbaum, H.-W. Hammer and U.-G. Meißner, Rev. Mod. Phys. **81** (2009) 1773 [arXiv:0811.1338 [nucl-th]].

[9] R. Machleidt and D. R. Entem, Phys. Rept. **503** (2011) 1 [arXiv:1105.2919 [nucl-th]].

[10] M. Lenkewitz, E. Epelbaum, H.-W. Hammer and U.-G. Meißner, Phys. Lett. B **700** (2011) 365 [arXiv:1103.3400 [nucl-th]].

[11] P. Argan *et al.*, Phys. Rev. C **21** (1980) 1416.

[12] P. Argan *et al.*, Phys. Lett. **206B** (1988) 4 [Erratum-ibid. B **213** (1988) 564].

[13] J. C. Bergstrom, R. Igarashi, J. M. Vogt, N. Kolb, R. E. Pywell, D. M. Skopik and E. J. Korkmaz, Phys. Rev. C **57** (1998) 3203.

[14] M. G. Barnett, R. Igarashi, R. E. Pywell and J. C. Bergstrom, Phys. Rev. C **77** (2008) 064601.

[15] D. Djukanovic, M. R. Schindler, J. Gegelia and S. Scherer, Phys. Rev. D **72** (2005) 045002. [hep-ph/0407170].

[16] A. N. Kvinikhidze, B. Blankleider, E. Epelbaum, C. Hanhart and M. P. Valderrama, Phys. Rev. C **80** (2009) 044004. [arXiv:0904.4128 [nucl-th]].

[17] E. Epelbaum, W. Glöckle, U.-G. Meißner, Eur. Phys. J. A **19** (2004) 125. [nucl-th/0304037].

[18] E. Epelbaum, W. Glöckle, U.-G. Meißner, Eur. Phys. J. A **19** (2004) 401. [nucl-th/0308010].

[19] S. Liebig, V. Baru, F. Ballout, C. Hanhart and A. Nogga, Eur. Phys. J. A **47** (2011) 69 [arXiv:1003.3826 [nucl-th]].

[20] A. Nogga, private communication.

[21] G.P. Lepage, J. Comp. Phys. **27** (1978) 192.

[22] G. P. Lepage, arXiv:nucl-th/9706029.

[23] E. Epelbaum and J. Gegelia, Eur. Phys. J. A **41** (2009) 341 [arXiv:0906.3822 [nucl-th]].

[24] C. Fernandez-Ramirez, A.M. Bernstein and T.W. Donnelly, Phys. Rev. C **80** (2009) 065201 [arXiv:0907.3463 [nucl-th]].

[25] H. Krebs, "Neutral pion electroproduction off the deuteron", Dissertation, University of Bonn (2003).

[26] V. Bernard, N. Kaiser and U.-G. Meißner, Nucl. Phys. A **607** (1996) 379 [Erratum-ibid. A **633** (1998) 695] [hep-ph/9601267].

[27] V. Bernard, N. Kaiser and U.-G. Meißner, Phys. Rev. Lett. **74** (1995) 3752 [hep-ph/9412282].

[28] V. Bernard, B. Kubis and U.-G. Meißner, Eur. Phys. J. A **25** (2005) 419 [nucl-th/0506023].

[29] A. Schmidt *et al.*, Phys. Rev. Lett. **87** (2001) 232501 [arXiv:nucl-ex/0105010].

[30] A. Gasparyan and M. F. M. Lutz, Nucl. Phys. A **848** (2010) 126 [arXiv:1003.3426 [hep-ph]].

[31] M. P. Rekalo and E. Tomasi-Gustafsson, Phys. Rev. C **66** (2002) 015203 [nucl-th/0112063].

[32] V. Baru, C. Hanhart, A. E. Kudryavtsev and U. G. Meißner, Phys. Lett. B **589** (2004) 118 [nucl-th/0402027].